

Iron Oxide Nanoparticles of *Cystoseira* sp. Sugar alcohol Treat MRSA and Thyroid gland cancer

By Doha Abou Baker

Iron Oxide Nanoparticles of *Cystoseira sp.* Sugar alcohol Treat MRSA and Thyroid gland cancer

Abstract

Purpose: Methicillin-resistant *Staphylococcus aureus* (MRSA) infections are emerging as a cause of suppurative thyroiditis. The resistance to several antibiotics and finding treatment has grown more difficult. Hence, the purpose of this study was to examine biosynthesized iron oxide nanostructures' antimicrobial activity as well as their cytotoxicity on normal and thyroid cancer cells. **Methods:** By using the sugar alcohols of *Cystoseira sp.*, the authors synthesized the advanced biosynthesis of iron oxide nanoparticles (COINs). An agar-well diffusion method and a broth dilution method were used to investigate COINs' antimicrobial activity against MRSA isolates. However, their cytotoxicity against normal and thyroid cancer cell lines was determined by the MTT (3-(4,5-dimethylthiazol-2-yl)-2,5-diphenyltetrazolium bromide) assay. **Results:** A GC-MS analysis of the dried *Cystoseira sp.* extract revealed a high percentage of D-mannitol, which is essential for the synthesis of spherical nanoparticles with a mean average size of 5.8 ± 0.8 nm. The COINs showed a higher inhibition zone (9-15 mm) for 66.6% of MRSA isolates, and the MIC of COINs was 256 $\mu\text{g/ml}$. The cell wall of these bacteria inhibits the absorption of COINs. As a result, a large concentration of COINs is required to restrict bacterial growth. Moreover, COINs have cytotoxicity on thyroid cancer cell proliferation and normal thyroid cell lines at IC₅₀s of 1.71 ± 0.1 and 25.9 ± 1.6 $\mu\text{g/ml}$, respectively. This can be due to the negative charge of sugar alcohols, which affect protein absorption and subsequent biological behaviors. **Conclusion:** The promising findings of this study are in favor of the creation of very small iron oxide nanostructures for therapy.

Keywords: MRSA, Iron oxide nanoparticles, *Cystoseira sp.*, sugar alcohols, thyroid cancer cell

Introduction

The thyroid gland is unusual for infections due to its massive circulatory supply, vast lymphoid drainage, high iodine levels, and anatomic encapsulation.¹In children and young adults, up to 92% of acute suppurative thyroiditis cases are discovered, most of which have anatomic alterations.²Acute suppurative thyroiditis symptoms comprise fever, dysphagia, and neck swelling. It foreshadowed upper respiratory illnesses.¹ Anaerobes, as well as gram-positive

Staphylococcus aureus, are the most common pathogens.³ The thyroid functions are usually normal in immunocompromised patients¹. However, thyrotoxicosis occurs when the destruction of the gland leads to the thyroid hormones' release into the bloodstream³.

Infection with methicillin-resistant *S. aureus* is becoming more common. It has also been identified as a significant pathogen in the infections of head and neck. Extensive PubMed investigation revealed less than 5 published cases of Methicillin-resistant *S. aureus* (MRSA) thyroid abscess.⁴⁻⁷ Recently, Hadid et al. (2015) displayed that cancer patients have a high risk of MRSA and blood stream infections, which increase the rate of mortality into 35-87%.⁸⁻⁹ MRSA infection is extremely difficult to treat because it has developed resistance to nearly all kinds of antibiotics, beginning with penicillin and , progressing to the most current, linezolid and daptomycin.¹⁰ As a consequence, its importance to advance novel therapeutic tactics. The fast progress of nanotechnology offers a hopeful solution to this predicament. Functional nanoformulations perform as antibacterials for MRSA infection.¹¹

In the future, humans will heavily rely on nanomaterials for their biomedical needs, and green nanomaterials have the advantage of being more biocompatible with human cells.¹²⁻¹⁵ In the biomedical field, magnetic nanoparticles are some of the most useful metal nanoparticles.¹⁴ Due to their magnetic properties, iron oxide nanoparticles have proven to be useful for reducing drug administration, detecting, guiding, and treating cancer.¹⁶

In this regard, seaweeds have also demonstrated very interesting bioactivities with their secondary metabolites, proteins, peptides, and pigments, which serve as nanofactories.¹⁷ This is the first research to investigate the antibacterial and anticancer properties of iron oxide nanoparticles produced by the brown marine alga *Cystoseira spp.* extract against Methicillin-resistant *S. aureus* and thyroid gland cancer. *Cystoseira spp.* extract contains a variety of useful chemicals, many of which are yet unknown. The study identifies the bioactive component that has role in formation of Iron oxide nanoparticulates.

Methods

Materials

Cystoseira spp. were collected from the coastal area of the Red Sea, Hurghada, Egypt, during January 2019 and identified in the Faculty of Science, Al Azhar University, Cairo, Egypt. TT Cancer thyroid cell lines and Nthy-ori 3-1 normal thyroid cell lines were received from Vacsera, Cairo, Egypt. The ferric chloride anhydrous (98%), Triton X-100, dimethyl sulfoxide (DMSO), Dulbecco's Modified Eagle Media (DMEM), p-iodonitrophenyltetrazolium violet, trifluoroacetic acid, acetonitrile, MTT salt, Muller-Hinton broth and agar (MHA), SD fine chemicals, Methicillin-resistant *S. aureus* (MRSA).

Preparation of *Cystoseira spp.* extract

Cystoseira spp. were cleaned and kept at -20 degrees Celsius. To prepare the aqueous extract, approximately 1 g was powdered, freeze-dried, and boiled with 100 mL of distilled deionized water for 15 minutes in an Erlenmeyer flask with while stirring constantly. The extract was then cooled to room temperature and filtered.

Biosynthesis of iron oxide Nanoparticles by *Cystoseira spp.* extract (CIONs)

The ferric chloride salt solution 0.2 M was added to an aqueous extract of *Cystoseira spp.* in an equal volume ratio, and then the mixture was stirred for one hour and permitted to locate at room temperature for half an hour.¹⁴

Gas chromatography–mass spectrometry analysis (GC-MS)

The dried extract was diluted in 20 μ l of pyridine and derivatized with 50 μ l of N,O-bis(trimethylsilyl)-trifluoroacetamide (BSTFA) for 60 minutes at 70°C. Then it was introduced into the GC/MS.¹⁸

Different components were identified by comparing their spectra fragmentation patterns to those recorded in Wiley and NIST Mass Spectral Library data.^{18,19}

Characterization of iron oxide Nanoparticles

Biosynthesized iron oxide nanoparticles were characterized via Fourier transform infrared spectroscopy (FTIR) (JASCO 4600), Two milligrams of CIONs and algae extract were mixed with 200 mg KBr (FT-IR grade) and pressed into a pellet. Then it located into the sample holder and FT-IR spectra were recorded in the range 3500–500 cm^{-1} . Also the reduction of iron ions was measured by U-visible spectroscopy (Shimadzu UV-2600) with digital data acquisition, and wavelength range 250– 450 nm. High-Resolution Transmission Electron Microscopy (HRTEM,

JEOL-JEM-2010) was used to detect the morphology, size and shape of CIONs. And the instrument was operated at an accelerating voltage of 200 kV. Drop-cast CIONs were dried under vacuum under carbon coated copper grids. Energy disperse X-ray (EDX) analysis of CIONs was carried using the same device to examine the element composition of CIONs.

Detection of Methicillin Resistant *S. aureus* (MRSA)

MRSA strains were received from the microbiology laboratories of Egyptian hospitals and detected in the Egyptian Drug Authority, Giza, Egypt. MRSA was detected with the use of a cefoxitin disk (30 µg) diffusion. The culture was done on a Mueller-Hinton agar plate with 0.5 McFarland standard of *S. aureus* broth. After allowing the lawn culture to dry for about 5 minutes, a cefoxitin disk (30 µg) was placed on top of it. Finally, the agar plate was incubated for 18 hours at 35° C. MRSA strains had a zone of inhibition diameter of less than 21 mm, whereas Methicillin-susceptible *S. aureus* strains had a zone of inhibition diameter of more than 22 mm.²⁰

Antibiotics susceptibility test for Methicillin resistant *S. aureus* (MRSA)

Antimicrobial sensitivity of nine MRSA isolates was detected by disk-diffusion method. Bacterial suspensions (0.5 McFarland tubes) of MRSA were inoculated on Mueller-Hinton agar. The antibiotic disks of 6-mm diameter were purchased from Oxoid, Basingstoke, UK; Amikacin (AMK) 30µg; Ceftriaxone (CRO) 30µg; Ampicillin / sulbactam (SAM) 10/10µg; amoxicillin/clavulanic acid (AUG) 20/10µg; Ceftazidime (CAZ) 30µg; cefoxitin (fox) 30µg; Ciprofloxacin (CIP) 5 µg; and cefotaxime (CAZ) 30µg; Erythromycin (E) 30µg; Vancomycin (VA) 30µg, and Linezolid (LAZ) 30µg were placed on the plates and incubated at 37°C for 24h. The diameter of inhibitory zone was determined in millimeters according to Masood et al. (2010), and the Clinical and Laboratory Standards Institute (CLSI 2012 and 2020).²⁰⁻²²

Screening for the antibacterial activity of *Cystoseira* sp Iron Oxide Nanoparticles (CIONs)

The antibacterial activity of iron oxide nanoparticles was investigated against nine clinical strains of methicillin-resistant *S. aureus* by using the agar-well diffusion method. The Muller Hinton Agar (MHA) plates were inoculated with 0.5 McFarland turbidity of MRSA according to the National Committee for Laboratory Standards (CLSI) for 2020 and 2012.²⁰⁻²² The antimicrobial activity was measured by measuring the inhibition zone using the Himedia Zone Reader.²³ MIC was determined as the lowest concentration of antimicrobial test substance as described previously by Balouiri et al. (2016), Makky et al. (2021)²⁴⁻²⁵

Cell viability assay

In 96-well microtiter plastic plates, we grew TT Cancer thyroid cell lines and Nthy-ori 3-1 normal thyroid cell lines for 24 h under 5% CO₂ in fresh complete growth medium. Cells were incubated either alone or with iron oxide nanoparticles to give a final concentration of 0.39, 1.56, 6.25, 25, and 100 µg. After 48 hours incubation, sodium dodecyl sulphate (SDS) was added to each well and incubated overnight at 37°C to dissolve the crystals. The absorbance at 595 nm on a microplate multi-well, 620 nm was used as the reference wavelength. MTT assay were performed as described by El-Menshawī et al. (2010)²⁶

Results

In the coastal area of the Egyptian Red Sea, *Cystoseira* brown algae (order Fucales, family Sargassaceae) have distinct basal and apical regions, and have air-vesicles. (Fig.1). Further, the main axis of *Cystoseira* spp. is elongated foliage, and their lowest sections, known as foliar expansions or basal leaves, are heavily flattened (Fig.1). In our study, iron oxide nanoparticles (CIONs) biosynthesized by allowing *Cystoseira* spp. water extract to react with 0.2 M FeCl₃ solution, and the reactions took place at room temperature. Consequently, the yellowish brown ferric chloride solution became a dark brown colloidal solution. The UV spectrum of CIONs was analyzed by using a UV-visible spectrophotometer (Fig.2). The absorbance peaks at 290 nm confirmed the formation of the monodispersed iron oxide nanoparticles.

The GC-MS profiling of the dried *Cystoseira* spp. extract showed three sugar alcohol compounds, including glycerol, dulcitol (galactitol), and D-mannitol, and the highest percentage was for D-mannitol (94.9%) (Fig.3). However, the percentages of glycerol and dulcitol in the extract were 1.41% and 3.6%, respectively.

Our intent was to identify the functional groups involved in the biosynthesis of iron oxide nanoparticles by comparing their IR spectrum with that of dried *Cystoseira* spp. (Fig. 4). The IR spectra of dried *Cystoseira* spp. extract indicated several functional groups as follows: 3450 cm⁻¹ represents the O-H group of sugar or alcohol, while 2900 cm⁻¹ indicates the existence of aliphatic C-H stretching vibrations. Further, 2494.8 cm⁻¹ and 1417 cm⁻¹ showed the presence of O-H bending alcohol, whereas 1050 cm⁻¹ proved the presence of C-O stretching vibration of alcohol. In addition, iron oxide nanoparticles displayed an intense absorption spectra for O-H at 3.380 cm⁻¹, and red shift were noticed for 2494.8 cm⁻¹, 1050 cm⁻¹ of O-H bending, and C-O stretching vibration alcohol to 2550 cm⁻¹, and 1110 cm⁻¹, respectively. A C=C stretching

vibration of conjugated alkene was also detected at 1,650 cm⁻¹. Our findings are consistent with recent GC mass spectroscopy data that demonstrated the presence of sugar alcohol in *Cystoseira* spp. extract.

The HRTEM images of CIONs revealed monodispersed spherical forms with sizes ranging from 4.62 nm to 7.62 nm, with a mean average size of 5.8 ±0.8 nm. (Fig5).

The structure of materials present in CIONs was examined ⁴ using EDX. The purity level of the nanoparticles was analyzed, which confirms that *Cystoseira* spp. extract-mediated iron oxide Nanoparticles have 31.6%±4.5 of iron, and 46.72%±4.4 of oxygen, respectively (Fig6). The Cl signals must originate from the ferric chloride precursor used in the protocol of biosynthesis. Also, other signals by elements such as Si, Cu, Zn, and Ca originated from the algae that mediated the biosynthesis. The presence of ⁴ iron and oxide peaks confirms the formation of iron oxide nanoparticles.

On Mueller Hinton agar plates, an antibiogram for different *Staphylococcus aureus* strains was assessed using the disk-diffusion technique and interpreted according to the CLSI guidelines. On the basis of resistance to third- and second-generation antibiotics such as ceftazidime, cefotaxime, and ceftriaxone, isolates were identified as MRSA during a multidrug-resistant (MDR) investigation. To confirm the presence of MRSA, the MDR pattern of the isolates was examined with different antibiotics from the cephalosporin and methicillin groups. All *Staphylococcus aureus* isolates were highly susceptible to vancomycin, linezolid (100%), amikacin (66.6%), and erythromycin (66.6%) (Table 1). They were highly resistant to amoxicillin + clavulanic acid (100%), ceftazidime, ampicillin/sulbactam, ceftriaxone (100%), erythromycin (66.6%), and ciprofloxacin (66.6%) (Table 1).

The antimicrobial activity of COINs nanosuspensions has been screened using the agar well diffusion technique. The COINs nanosuspensions showed higher antimicrobial activity against MRSA isolates compared to DMSO alone and the aqueous *Cystoseira* spp. extract (Fig. 7a). The COINs nanosuspensions showed an inhibition zone (9–15 mm) for 66.6% of MRSA isolates, as shown in Fig. 7b. However, the inhibition zones of amikacin, linezolid, vancomycin, and, in some cases, erythromycin and ciprofloxacin were higher (14–21 mm).

According to the microdilution method, the growth of MRSA ⁵ was decreased when it was cultured with 128, 256, and 512 $\mu\text{g/ml}$ of COINs. Visual examination of bacterial growth as turbidity or pellets in the wells of the microtiter plate to determine the minimum inhibitory concentration is difficult. Colorimetric approaches are appealing because they have the ability to produce distinct endpoints based on a visible color shift. The tetrazolium salt p-iodonitrophenyltetrazolium violet (INT) was used as a bacterial growth indicator for our study. INT is a chemical that is converted to a violet INT formazan product by bacterial dehydrogenases in metabolically active bacterial cells, as in 128 to 256 $\mu\text{g/ml}$ of COINs concentrations and the negative control (Fig.7c). The minimum inhibitory concentration of COINs by 100% to 256 $\mu\text{g/ml}$ for 88.8% of MRSA isolates and to 128 $\mu\text{g/ml}$ for 11.1% of MRSA isolates.

Till now, there has been no study on the effect of iron oxide nanoparticulates on thyroid cancer. Thyroid carcinoma is the most prevalent malignant tumor of the human endocrine system. The ²⁰ MTT assay was used to investigate the effects of COINs on the viability of TT cancer ¹ thyroid cell lines and N thy-ori 3-1 normal thyroid cell lines. The concentration of COINs that lowers cell viability by 50% (IC_{50}) was found to be $1.71 \pm 0.1 \mu\text{g/ml}$ in TT cell lines. However, for N thy-ori 3-1 cell lines, IC_{50} was observed at $25.9 \pm 1.6 \mu\text{g/ml}$. Moreover, the toxicity of COINs was observed on normal cell lines at high concentrations ($25.9 \pm 1.6 \mu\text{g/ml}$) compared to staurosporine ($16.2 \pm 0.9 \mu\text{g/ml}$) (Table 2 & Fig. 8).

Discussion

Cystoseira members produce a wide range of potentially bioactive substances, including terpenoids, fatty acids, triacylglycerols, steroids, phlorotannins, and polysaccharides, which highlight the genus' importance.²⁷

The UV absorbance peak of COINs at 290 nm ⁹ agreed with the absorption peaks of iron oxide nanoparticles by Das et al., 2014 and Abbas et al., 2020.^{28,14} The mechanism of iron oxide nanoparticles depends on the biologically active metabolites of the *Cystoseira spp.* water extract, such as carbohydrates or sugar alcohols, which are detected by GC mass spectroscopy. Mannitol is a type of sugar alcohol, or polyol, that is produced from the reduction of carbohydrates and is in control of osmoregulation in macroalgae²⁹. Similar to our results, Andrade et al., 2012 detected that *Cystoseira* species are rich sources of mannitol.³⁰ Further, Pell and coworkers

(2013) found glycerol-arsenosugar in the brown algae *Cystoseira spp.*³¹ It's known that sugar alcohols act as scavengers of reactive oxygen species, thereby avoiding the peroxidation of lipids and consequently destroying cells.³² The IR and GC mass spectroscopy indicate that sugar alcohols (especially mannitol) ¹ over the surface of COINs were the cause of the synthesis and stabilization of CIONs. In this regard, Gawali et al. (2017) use D-mannitol as a coat for the stabilization of iron oxide nanoparticles, which are prepared chemically by coprecipitation.³³ This is the first work to prove the role of mannitol and other sugar alcohols in the *Cystoseira spp.* extract in the biosynthesis and stabilization of iron oxide nanoparticles.

For COINs Characterization Similarly, Ur Rahman et al., 2017 confirmed ¹⁴ the atomic percentages received from EDX quantification were 48.98% of O, 8.83% of Fe. Also, they explained the origin of the Cl signal was Fe (NO₃)₃·9H₂O precursor and the gooseberry leaf extract used for the synthesis of nanoparticles.³⁴

On the basis of MRSA resistance, similarly, Sabir et al. (2014) showed that MRSA pathogens have high susceptibility to vancomycin (100%) and erythromycin. In addition, fifty percent of the Ciprofloxacin MRSA resistance was isolated in Indian literature.³⁵

Recently, ZnO nanoparticles, CuO nanoparticles, and α -Fe₂O₃ have been revealed to exhibit antimicrobial potential, which comes in agreement with our study.^{36,14} The proper explanation for why the inhibition of MRSA growth needs high concentrations of COINs may be that the ²⁵ outer cell wall of gram-positive bacteria contains a thick peptidoglycan ⁶ coating that acts as a barrier against most inhibitory compounds and leads to the hard absorption of iron nanoparticles.³⁷

Furthermore, ⁶ the antibacterial efficiency of iron oxide- nanoparticles may be influenced by the reaction between ions released from nanomaterials and proteins with thiol groups (-SH) on the bacterial cell surface.³⁸ For the higher inhibition zones of amikacin, linezolid, vancomycin, and, in some cases, ciprofloxacin compared to the inhibition zones of COINs, we recommended in future studies the combination of antibiotics with COIN, which may have a synergistic effect to combat MRSA infection. It was reported by Abbas et al. that iron oxide nanoparticles cause morphological modifications and shape distortion in cancer cell lines.¹⁴

The cytotoxic effect of low doses of COINs can be explained by the charge of coating materials (as sugar alcohols), which are provided on iron oxide nanoparticles, which may change the surface charge of the nanoparticles, affecting protein absorption and subsequent biological behaviors.³⁹ Xiao et al., for example, found that strongly positive or negatively charged micellar nanoparticles were substantially absorbed by macrophages in the liver, whereas slightly negative-charged nanoparticles had the lowest macrophage absorption and the maximum tumor uptake, which comes in agreement with our study.⁴⁰ Biological stabilizing molecules, play an essential role in determining the toxic nature of metal nanoparticles. There is also a variation in the toxic nature of nanomaterials depending on their size, reductants, and capping materials.⁴⁰ It can be concluded from the above facts that, depending on how nanomaterials are synthesized, the toxic nature of the nanomaterial will differ. Moreover, to overcome antibiotic resistance and enhance their efficacy, COINs can be combined with antibiotics. Antibiotics can be taken at a lower dose and with less toxicity when they are taken with them⁴⁰. Future in vivo studies of COINs are highly recommended to evaluate their toxicity and therapeutic purposes against MRSA infection.

Conclusion

The biogenic fabrication of iron oxide nanoparticles using sugar alcohol from *Cystoseira spp.* extract is the technique presented in this study. The high concentration of these nanoparticles was found to display antimicrobial activity against Methicillin-resistant *Staphylococcus aureus*. The thick peptidoglycan coatings on their outer cell walls act as a barrier against most inhibitory compounds and allow iron nanoparticles to be absorbed well. For that reason, the suppression of bacterial growth needs a high concentration of these nanoparticles. Furthermore, the cytotoxic effect of nanoparticles against thyroid normal cell lines and thyroid cancer cell lines in low doses could explained by the negative charge of sugar alcohols coated the nanoparticles, which affect protein absorption and subsequent biological behaviors. Future in vivo studies for the cytotoxic effect of these nanoparticles against thyroid cancer and MRSA infection are recommended.

Conflict of interest

This research was conducted without any commercial or financial relationships that could be construed as potential conflicts of interest

Funding

This study wasn't supported by any fund.

Figures Ligands

Figure 1. *Cystoseira sp.* collected from the coastal area of the Egyptian red sea.

Figure 2. UV spectrum of iron oxide Nanoparticles (black line) biosynthesized by *Cystoseira sp.* a: ferric chloride solution, and b: iron oxide nanosuspension.

Figure 3. GC-MS Profiling of the dried *Cystoseira sp.* water extract.

Figure 4. FTIR of the dried *Cystoseira sp.* water extract (A) and biosynthesized iron oxide Nanoparticles (B).

Figure 5. HRTEM micrograph of *Cystoseira sp.* extract mediated iron oxide Nanoparticles (CIONs).

Figure 6. Energy Disperse Xray for *Cystoseira sp.* extract mediated iron oxide Nanoparticles (CIONs).

Figure 7. Antimicrobial activities of COINS Against MRSA Isolates

(a) By using agar diffusion method, (b) Against MRSA no. 4, 1: COINs, 2: DMSO, 3: Algae water extract, (c) MIC determination with INT dye; 1:8 lanes are 512 to 2 μ g COINs with MRSA, and 9 lanes are MRSA isolate as negative control



Fig.1. *Cystoseira* spp. collected from the coastal area of the Egyptian red sea.

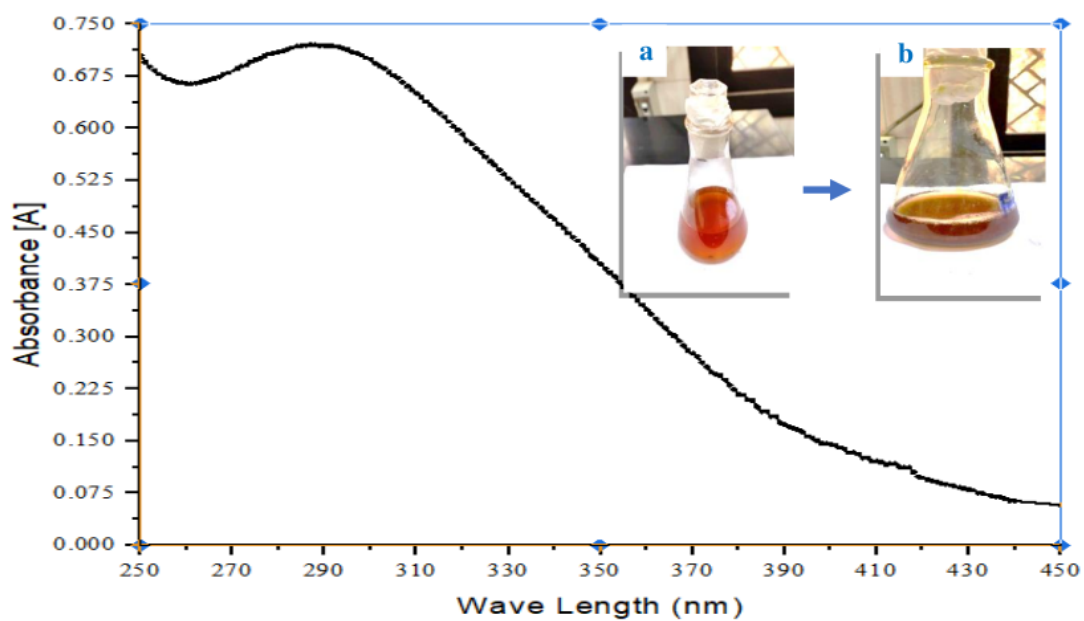


Fig. 2. UV spectrum of iron oxide NPs (black line) biosynthesized by *Cystoseira sp.* a: ferric chloride solution, and b: iron oxide nanosuspension.

Table (1) Compounds identified from *Cystoseira sp.* extract.

S.N	Peak Name	Retention Time	Peak Hight	Peak area	% Area
1	Glycerol 3TMS derivatives Formula: C ₁₂ H ₃₂ O ₃ Si ₃ Molecular weight: 308.6372	11.295	383316.08	635479.04	1.41
2	Dulcitol 6TMS derivatives Formula: C ₂₄ H ₆₂ O ₆ Si ₆ Molecular weight: 615.2585	18.898	975608.19	1615390.68	3.6
3	D -Mannitol 6TMS Formula: C ₂₄ H ₆₂ O ₆ Si ₆ Molecular weight: 615.3	18.974	20631583.12	42529543.33	94.9

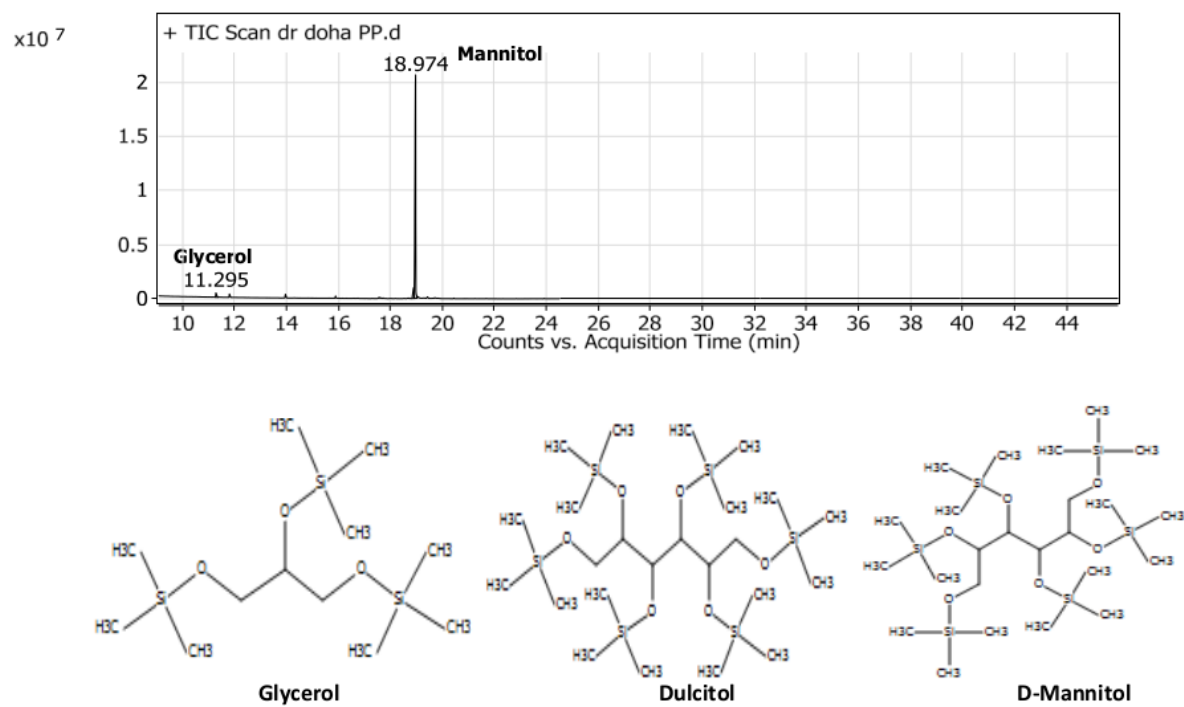


Fig.3.GC-MS Profiling of the dried *Cystoseira sp.* water extract.

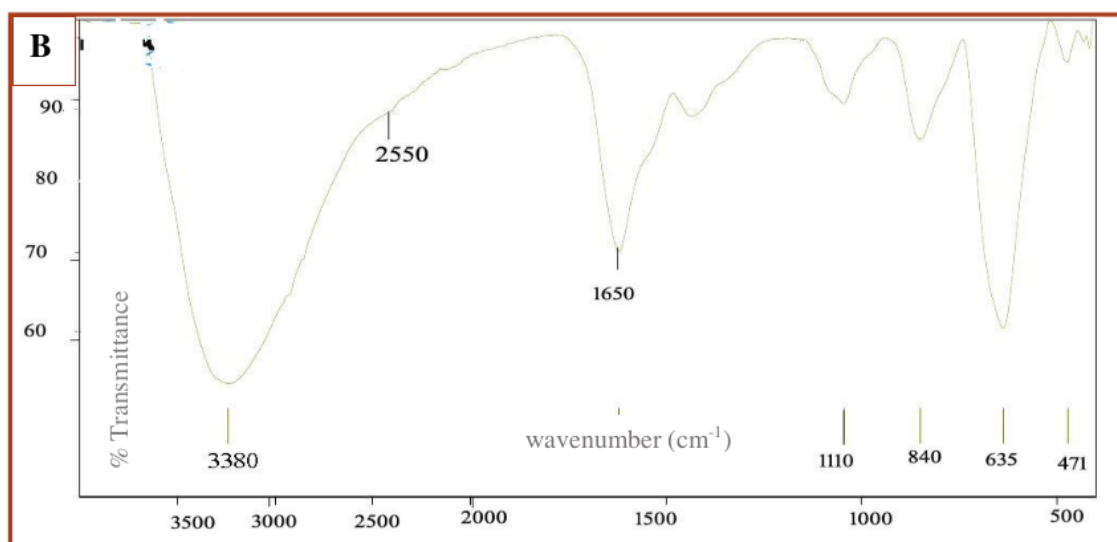


Fig.4.FTIR of the dried *Cystoseira sp.* water extract (A) and biosynthesized iron oxide NPs (B).

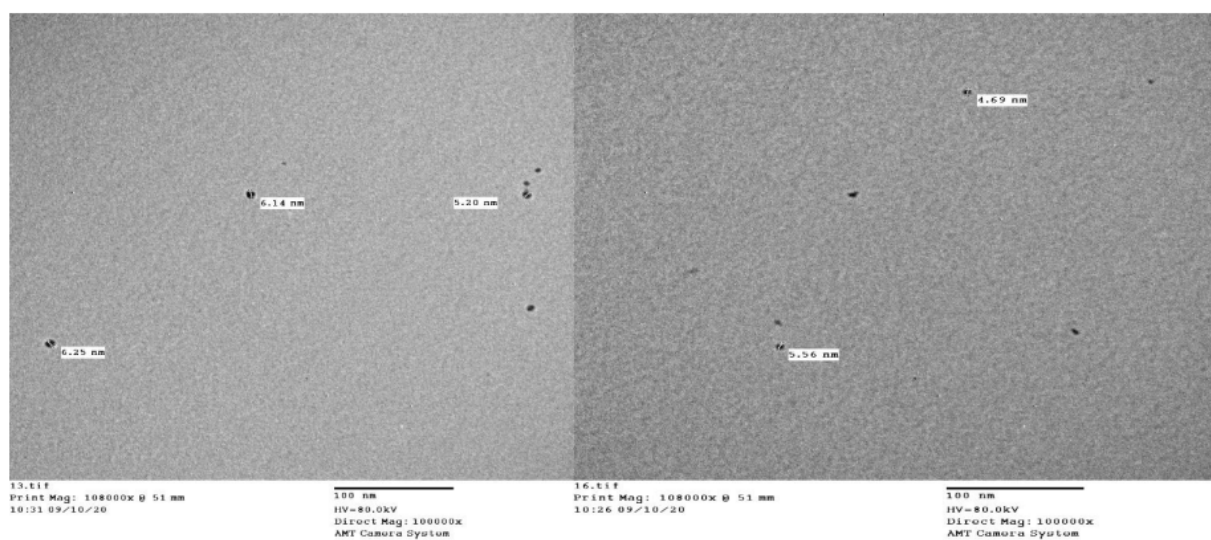


Fig.5. HRTEM micrograph of *Cystoseira sp.* extract mediated iron oxide NPs(CIONS).

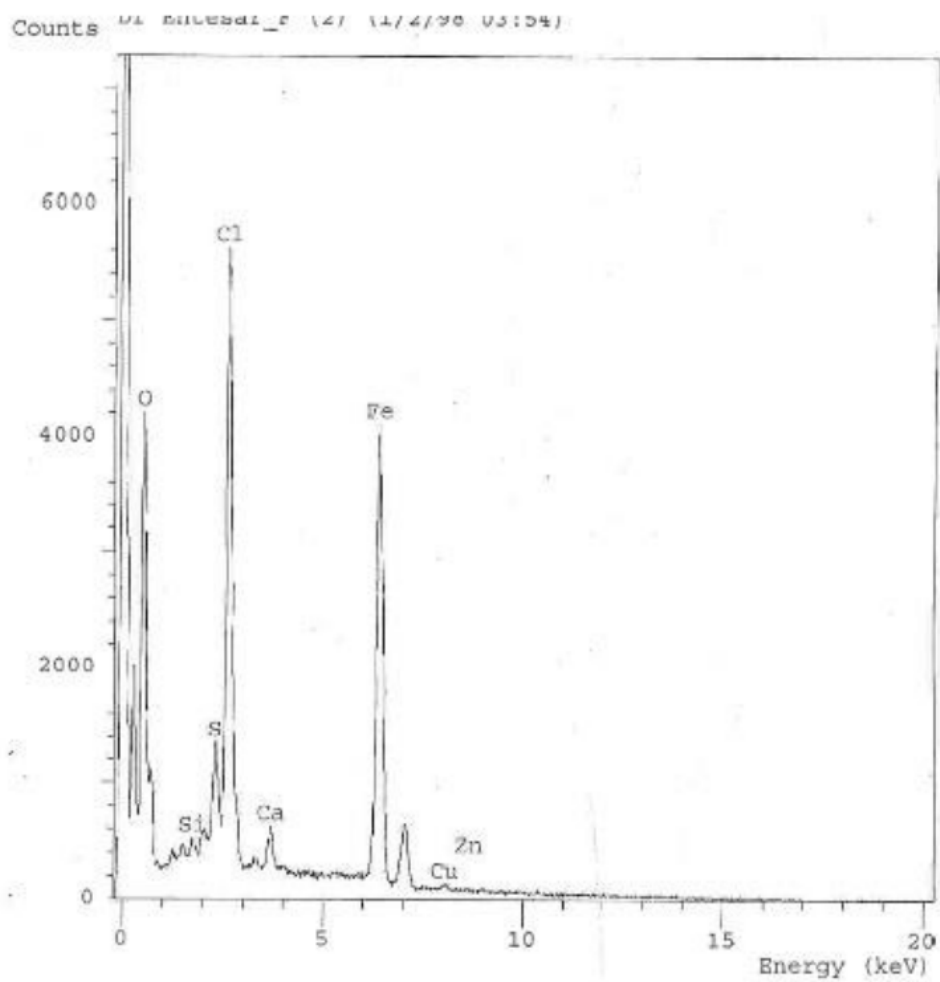


Fig. 6. Energy Disperse Xray for *Cystoseira trinodis* extract mediated iron oxide NPs (CIONs).

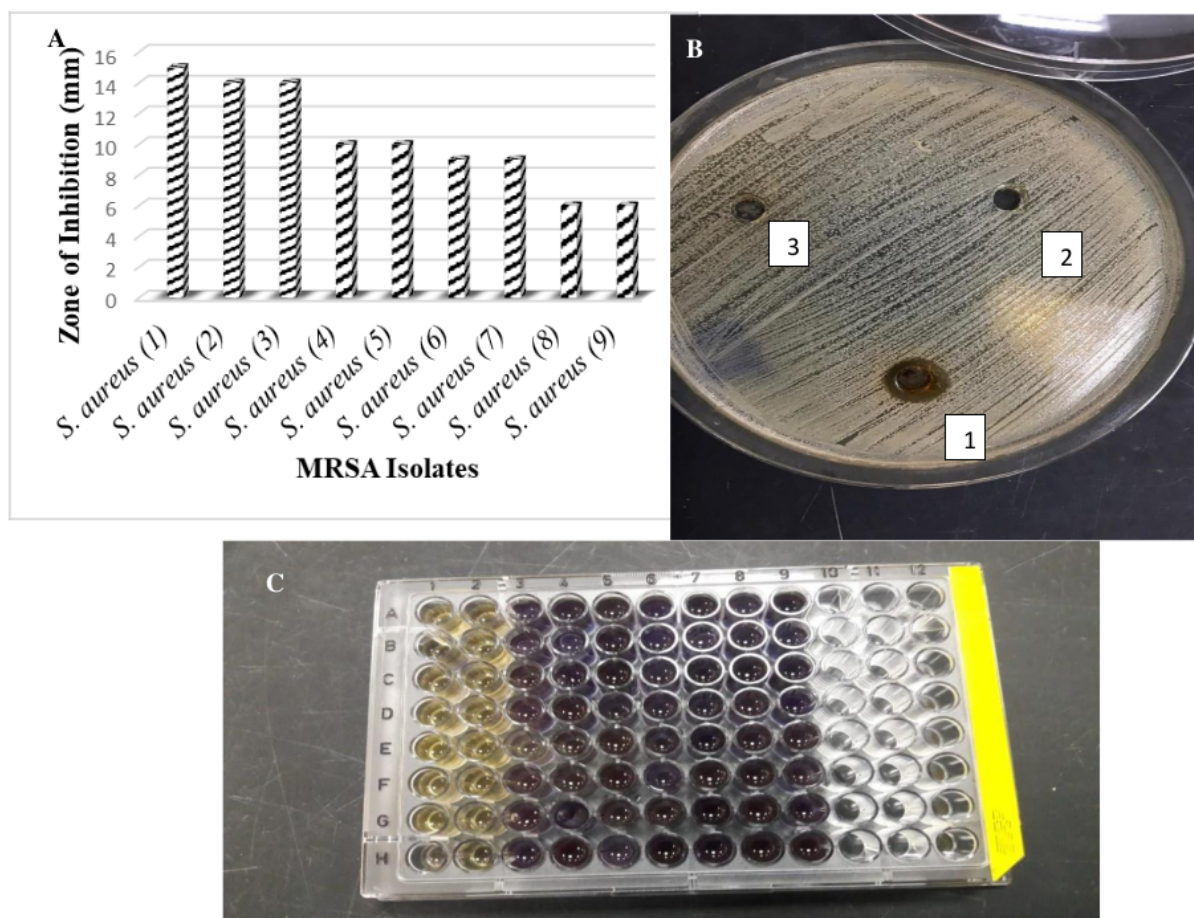


Fig.7. Antimicrobial activities of COINS Against MRSA Isolates

(a) By using agar diffusion method, (b) Against MRSA no. 4, 1: COINS, 2: DMSO, 3: Algae water extract, (c) MIC determination with INT dye; 1:8 lanes are 512 to 2 μ g COINS with MRSA, and 9 lanes are MRSA isolate as negative control

Table (2) Antibigram for different *Staphylococcus aureus* strains by using the disk-diffusion technique.

Antibiotics	Antibiotics Family	⁸ <i>S. aureus</i> (1)	<i>S. aureus</i> (2)	<i>S. aureus</i> (3)	<i>S. aureus</i> (4)	¹³ <i>S. aureus</i> (5)	<i>S. aureus</i> (6)	<i>S. aureus</i> (7)	<i>S. aureus</i> (8)	<i>S. aureus</i> (9)
Amikacin (AMK)	Aminoglycosides	R*	S*	S	S	R	R	S	S	S
Amoxicillin + clavulanic acid (AUG)	Aminopenicillin	R	R	R	R	R	R	R	R	R
Cefoxitin (FOX)	2nd generation cephalosporin	⁷ R	R	R	R	R	R	R	R	R
Ampicillin/sulbactam (SAM)	Aminopenicillin	¹¹ R	R	R	R	R	R	R	R	R
Erythromycin (E)	Macrolides	R	S	S	R	R	R	R	R	R
Vancomycin (VA)	Glycopeptide	²⁴ S	S	S	S	S	S	S	S	S
Cefotaxime (CTX)	3rd generation cephalosporin	R	R	R	R	R	R	R	R	R
Ceftriaxone (CRO)	3rd generation cephalosporin	⁷ R	R	R	R	R	R	R	R	R

Ciprofloxacin (CIP)	Fluoroquinolone	S	S	S	R	R	R	R	R	R
------------------------	-----------------	---	---	---	---	---	---	---	---	---

(*) R: resistant, and S: sensitive.

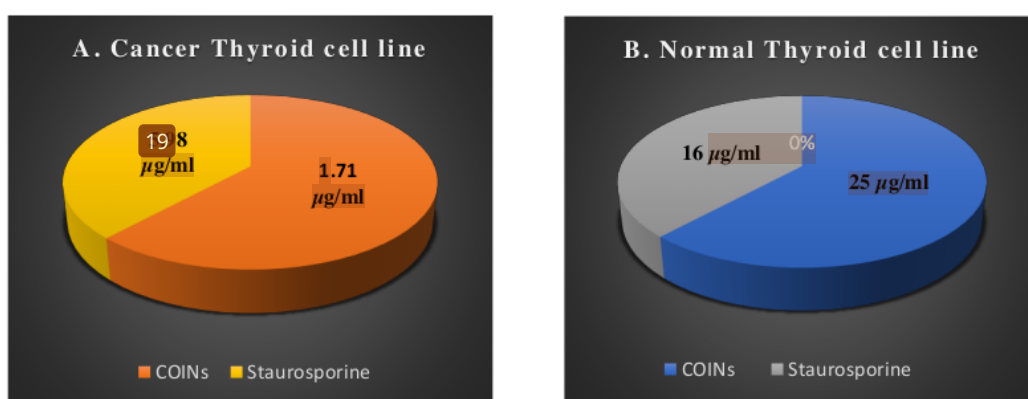


Fig.8. IC₅₀ of COINs and Staurosporine against cancer and normal thyroid cell lines.

Iron Oxide Nanoparticles of Cystoseira sp. Sugar alcohol Treat MRSA and Thyroid gland cancer

ORIGINALITY REPORT

15%

SIMILARITY INDEX

PRIMARY SOURCES

- | | | |
|---|--|----------------|
| 1 | link.springer.com
Internet | 123 words — 3% |
| 2 | www.researchsquare.com
Internet | 65 words — 2% |
| 3 | www.frontiersin.org
Internet | 41 words — 1% |
| 4 | P. Rajiv, B. Bavadharani, M. Naveen Kumar, P. Vanathi. "Synthesis and characterization of biogenic iron oxide nanoparticles using green chemistry approach and evaluating their biological activities", Biocatalysis and Agricultural Biotechnology, 2017
Crossref | 35 words — 1% |
| 5 | Heba Salah Abbas, Akilandeswari Krishnan, Muddukrishnaiah Kotakonda. "Antifungal and antiovarian cancer properties of α Fe ₂ O ₃ and α Fe ₂ O ₃ /ZnO nanostructures synthesised by <i>Spirulina platensis</i> ", IET Nanobiotechnology, 2020
Crossref | 31 words — 1% |
| 6 | Dalia M.S.A. Salem, Mona M. Ismail, Mohamed A. Aly-Eldeen. "Biogenic synthesis and antimicrobial potency of iron oxide (Fe ₃ O ₄) nanoparticles using algae | 26 words — 1% |

-
- 7 journals.tubitak.gov.tr 26 words — 1 %
Internet
-
- 8 scholar.ppu.edu 26 words — 1 %
Internet
-
- 9 Heba Abbas, Akilandeswari kraishnaiah, Muddukrishnaiah K. "The Antifungal and Antiovarian cancer properties of α Fe₂O₃ and α Fe₂O₃/ZnO nanostructures Synthesized by *Spirulina platensis*", IET Nanobiotechnology, 2020 25 words — 1 %
Crossref
-
- 10 tessera.spandidos-publications.com 20 words — < 1 %
Internet
-
- 11 Hellyar, A.G.. "Experience with *Nocardia asteroides* in renal transplant recipients", Journal of Hospital Infection, 198807 19 words — < 1 %
Crossref
-
- 12 www.plantphysiol.org 17 words — < 1 %
Internet
-
- 13 www.hindawi.com 16 words — < 1 %
Internet
-
- 14 www.researchgate.net 15 words — < 1 %
Internet
-
- 15 Che-Lun Chen, Chih-Wen Chi, Chen-Yi Lee, Yi-Ling Tsai, Uma Kasimayan, Mahesh K.P.O., Hong-Ping Lin, Yu-Chih Chiang. "Effects of surface treatments of bioactive 14 words — < 1 %

tricalcium silicate-based restorative material on the bond strength to resin composite", Dental Materials, 2023

Crossref

-
- 16 addi.ehu.es 13 words — < 1%
Internet
-
- 17 www.aensiweb.net 12 words — < 1%
Internet
-
- 18 www.cureus.com 12 words — < 1%
Internet
-
- 19 Rodrigues, Rúben Miguel Lopes. "Suberin Biotech Potential: From Bactericidal Nanoparticles to Optical Sensors", Universidade NOVA de Lisboa (Portugal), 2024 11 words — < 1%
ProQuest
-
- 20 Venkataraman Deepak, Paneer Selvam Umamaheshwaran, Kandasamy Guhan, Raja Amrisa Nanthini et al. "Synthesis of gold and silver nanoparticles using purified URAK", Colloids and Surfaces B: Biointerfaces, 2011 11 words — < 1%
Crossref
-
- 21 www.asianjab.com 11 words — < 1%
Internet
-
- 22 G. Jagathesan, P. Rajiv. "Biosynthesis and characterization of iron oxide nanoparticles using Eichhornia crassipes leaf extract and assessing their antibacterial activity", Biocatalysis and Agricultural Biotechnology, 2018 10 words — < 1%
Crossref

23	Hacene Boussafel, Charafeddine Sedrati, Safia Alleg. "Green synthesis of NiFe ₂ O ₄ , CoFe ₂ O ₄ , and Ni _{0.5} Co _{0.5} Fe ₂ O ₄ by sol-gel autocombustion method using olive leaf extract as fuel", Applied Physics A, 2024	10 words — < 1%
----	---	-----------------

Crossref

24	html.scirp.org	10 words — < 1%
----	--	-----------------

Internet

25	recerc.eu	10 words — < 1%
----	--	-----------------

Internet

26	www.ncbi.nlm.nih.gov	10 words — < 1%
----	--	-----------------

Internet

EXCLUDE QUOTES ON

EXCLUDE BIBLIOGRAPHY ON

EXCLUDE SOURCES

EXCLUDE MATCHES

OFF

< 10 WORDS